A Study of The Height of Suspension of Lightweight Objects in A Steady Air Stream

Botao Wei

Department of Earth Sciences and Engineering Southwest Jiaotong University ChengDu, China

wbt2022114785@my.swjtu.edu.cn

Abstract. The ongoing advancement of fluid mechanics has led to its implementation in a multitude of fields, including aerospace and agriculture. Nevertheless, there remains a gap in the study of the steady-state levitation height of lightweight objects. The objective of this study is to examine the correlation between the levitation heights of diverse lightweight objects in a steady state and their respective masses, dimensions, and shapes. Furthermore, the study will compare experimental data with theoretical data and utilize computational fluid dynamics (CFD) simulation to ascertain the drag coefficients. It was found that the levitation position of the sphere is inversely proportional to the sphere's own weight, directly proportional to the characteristic area of the gas flowing through the sphere (represent by the sphere's diameter in the experiments), and directly proportional to the approaching flow velocity. Additionally, the resistance of the CFD simulation was found to be close to the self-gravity force, which serves to verify the accuracy of the physical model.

Keywords: lightweight objects, drag, suspension, height, CFD.

1. Introduction

The aerodynamics plays an important role in various fields, including agricultural machinery [1-2], industrial separation technologies [3-4], and engineering design, especially in material separation and enhancing operational efficiency [5-7]. In agriculture, studies on the aerodynamic properties of walnut materials and the aerodynamic characteristics of cabbage seed separation have provided essential theoretical foundations and practical guidance for improving crop separation equipment [8]. By reading the experimental research, the researcher found that selecting an appropriate airflow speed can significantly enhance the efficiency of agricultural material separation [9]. However, despite the fact that these studies have identified optimal airflow speeds for different materials (such as walnut shells and seeds), the reasons why these specific airflow speeds are most effective have yet to be fully proved. In other words, while empirical data suggest that a particular wind speed achieves the best separation efficiency, there is a lack of scientific explanation for why these crops are better. In these studies, factors such as drag, lift, and turbulence effects are vital for understanding the behavior of materials in airflow.

With the rapid development of aerodynamics, research on the motion characteristics of balls such as ping-pong balls, soccer balls, and badminton during their movement has become increasingly advanced [10]. Also, a review of previous studies said that in a simplified two-dimensional model, a lightweight ball exposed to a stable airflow near its edge will experience a pullback due to the pressure gradient [11]. This experiment primarily investigates the horizontal deviation of the ball during its motion and explains why the ball can return to the center at the edge. But it does not explore the vertical suspension height of the ball and its stability in relation to factors such as airflow velocity and sizes.

In summary, the existing research on lightweight objects in the vertical direction is not very clear, and the data are mostly derived from empirical data, so this experiment is very meaningful for research. The objective of this experiment is to elucidate how the equilibrium between gravity and drag facilitates the stable suspension of lightweight objects, such as ping-pong balls. This experiment specifically intends to investigate the vertical dynamics of a lightweight item in airflow, concentrating on the impacts of steady airflow at a designated speed, drag, turbulence, and jet behavior on the motion of a ping-pong ball. This equilibrium is both a physical phenomenon and has practical applications in many engineering contexts where fluid flow interacts with lightweight things.

This experiment first uses 3D printing technology to change the quality and size of the ball, adjusts different wind speeds through the hairdryer to stabilize the ball at different heights, records the video, and then measures the distance through the tracker software, calculates the change of distance data over time, and records the average value. And compare the results with the theoretical values got from the Bernoulli's equation to attest to the drag theory model and get a better understanding of the interactions between fluid dynamics and lightweight object motion. This was used as the basis for CFD simulations, which were used to derive the drag coefficient of the sphere. Additionally, experiments will also be conducted with non-spherical objects to further explore the dynamics of objects in upward vertical turbulence. This research not only provides empirical data for basic aerodynamics but also offers new perspectives on issues related to industrial separation technologies and the control of moving objects.

2. Method

2.1. Experimental Model

The experiment utilizes an infinitely large space filled with air as the control volume, within which a circular inlet of diameter is defined at a specific location on the bottom boundary of the control volume. A steady jet issuing from the inlet provides fluid with a certain initial velocity; this fluid collides with and flows around a sphere of diameter, imparting an aerodynamic drag force on the sphere. When the aerodynamic drag force balances the sphere's own weight, the sphere remains suspended within the infinitely large air control volume. In this model, both the sphere's weight and diameter are variable, as is the inlet flow velocity. The model is depicted in Fig. 1.

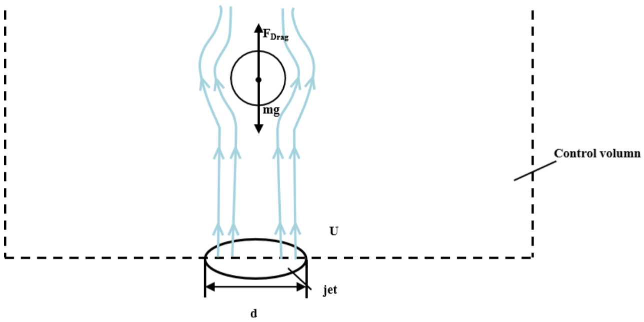

Fig .1. Physical Model of Ball Levitation

2.2. Experimental Objectives

By measuring the inlet wind speed, inlet diameter, the distance of the sphere from the inlet, and the sphere's weight and diameter, we calculate the theoretical levitation position of the sphere using the drag force equation and the variation of approach flow velocity with distance. We then compare this theoretical value with the actual measured value and calculate the error. This process serves to verify the aerodynamic principles.

2.3. Methodology

According to the above experimental model, when the air velocity of the hair dryer nozzle is large enough, the ball is suspended, and the product of its acceleration and mass is equal to the combined external force according to Newton's second law:

$$\sum F = ma \tag{1}$$

Then, substituting the expression of weight and (1) into the equation,

$$F_{\text{Drag}} - mg = 0 \tag{2}$$

Expand the resistance expression

$$F_{\text{Drag}} = \frac{1}{2} C_d \rho S v^2 \tag{3}$$

In addition to the equilibrium between the volume force of the research object and the differential pressure resistance caused by aerodynamics, it is also necessary to introduce the Reynolds number and the flow velocity calculation formulas of the center jet at different positions in the above-mentioned turbulence hypothetical model and jet velocity model in this experiment, which are listed here:

$$Re = \frac{\rho U d}{\mu} \tag{4}$$

$$U(0, r) = \overline{U}_{\max} = \frac{5Ud}{x} \tag{5}$$

2.4. Material Preparation

Hairdryer (with low, medium, and high-speed settings), table tennis balls, 3D printed hollow spheres, vernier caliper, electronic scale, camera, tape measure, and tracking software Tracker.

2.5. Determination of Experimental Variable Data

1) Pellet Mass: In order to vary the mass of the ball while maintaining its diameter, three-dimensional printing was employed with materials of varying densities. The diameter of the ball was maintained at 40mm, with the mass altered by the selection of the material. The effect on volume was deemed to be insignificant.

2) Diameter: In order to alter the dimensions of the ball without affecting its mass, a 35mm diameter ball was 3D printed using PC material. The smaller ball, designated D1, exhibited properties comparable to those of a standard table tennis ball.

3) Wind Speed: The wind speed was varied by adjusting the hairdryer's gear to change the airflow, while maintaining the mass and volume of the ball at a constant level. The standard table tennis ball, designated Ball A, was employed to investigate the impact of wind speed, with the resulting data from the experiment utilized for calculations.

2.6. Suspension Height Measurement

Conduct experiments. Take a video of the object is suspended in the air. The video is imported into Tracker software to measure the distance, record the distance data with time and calculate the average. As the flow is turbulent, and this experiment is under a realistic condition with many uncertainties, the object is not perfectly stable, which means that it wobbles both continuously and randomly. However, the fluctuation is still within a certain range. By using Tracker to grab the ball’s position either automatically or manually, the levitation height will be giving as a set of changing numbers. The distance x0 will be the average value of these numbers.

2.7. Repeat the Experiment

Experiments with different weights, different diameters, and different wind speeds on the same sphere were repeated, and each experiment was repeated at least three times to reduce accidental errors. Repeat the experiment with other shapes of objects and compare them with the results of the spheres. The experimenters drew the geometry of a cube and another egg-shaped and 3D printed it. The first wind speed was used for the experiment.

2.8. CFD Simulation

Based on the Ansys software Fluent module, the aerodynamic simulation analysis of the physical model was carried out, and the velocity contour diagram and pressure contour diagram were obtained.

3. Results

3.1. Collation of experimental data

1) Experiments-Ⅰ in Which the Height Changes with the Mass of the Pellets:

Table. 1 THEORETICAL HEIGHTS FOR DIFFERENT MASSES

Object	Ball A	Ball M1	Ball M2	Ball M3
Mass(g)	2.73	3.44	3.08	5.23
Experimental height (mm)	227.88	202.34	215.47	178.52

2) Experiments-Ⅱ in Which the Height Changes with the Diameter of the Pellets:

Table. 2 THEORETICAL HEIGHTS FOR DIFFERENT DIAMETERS

Object	Ball A	Ball D1
Diameter(mm)	40	35
Experimental height (mm)	227.88	204.19

3) Experiments-Ⅲ in Which the Height Changes with the Velocity of the Jet: Ball A (the ping-pong ball) was always selected as the research object.

Table. 3 THEORETICAL HEIGHTS FOR DIFFERENT VELOCITIES

Gear	1	2	3
U(m/s)	11.75	9.86	8.22
Theoretical height (mm)	238.48	218.37	199.45

3.2. Theoretical Calculations

In (1), μ is at 1 atmospheric pressure and 20℃, and the density of air is. The hairdryer flow speed ranges from 8.22 m/s to 11.75 m/s. In this case, the diameter of the hairdryer vent is 38.0 mm. Accordingly, re has a range from 20824 to 29766.67. It is within the range of 5000 to 200000, so the flow is turbulent flow, and the drag coefficient of the sphere is approximately 0.4. In this case, the Bernoullis equation,

$$P_1 + \frac{1}{2}\rho V_1^2 + \rho g z_1 = P_2 + \frac{1}{2}\rho V_2^2 + \rho g z_2 \tag{6}$$

Because the viscous effect of the fluid is strong under such low Reynolds number conditions, Bernoulli's law is more accurate when applied to stable conditions with no viscosity or very little viscosity. In fact, the ball can levitate in the flow field because of the pressure difference. When the relative airflow flows through the wall of the small ball, the airflow at its leading edge is blocked, the flow velocity slows down, and the pressure increases. The airflow at the trailing edge of the ball separates, forming a vortex zone and reducing the pressure. In this way, a pressure difference is created between the front and back of the ball to form resistance. This resistance is called differential pressure resistance. According to the formula for calculating the differential pressure resistance,

$$F_{\text{Drag}} = \frac{1}{2}C_d \rho S v^2 \tag{7}$$

In order for the ball to be suspended, the differential pressure resistance must be equal to the weight of the ball, so we can infer it,

$$\frac{1}{2}C_d \rho S U_{\max}{}^2 = mg \tag{8}$$

so, the expression for the exported velocity, is

$$U_{\max} = \sqrt{\frac{mg}{\frac{1}{2} C_d \rho \pi \left(\frac{1}{2}\mathrm{D}\right)^2}}. \tag{9}$$

At the same time, we can obtain the expression of velocity from the turbulent jet model mentioned in (5), which is coupled with the velocity expression of the differential pressure resistance above,

$$x = \frac{5U_{\mathrm{vent}}\mathrm{d}}{\sqrt{\frac{mg}{\frac{1}{2} C_d \rho \pi \left(\frac{1}{2}\mathrm{D}\right)^2}}} \tag{10}$$

In this way, we get the theoretical expression for the suspended position X.The relationship between the theoretical value and the variable is also plotted as a curve and compared with the experimental value, as shown in Figure. 2 to 4.

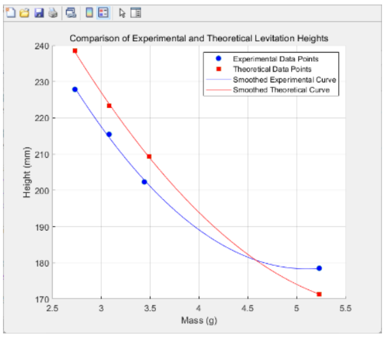

Fig. 2. Experimental and Theoretical Heights for Different Masses

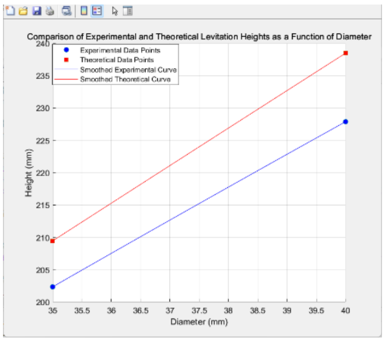

Fig. 3. Experimental and Theoretical Heights for Different Diameters

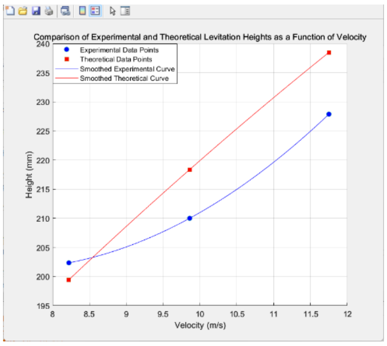

Fig. 4. Experimental and Theoretical Heights for Different Velocities.

For regular hexahedron, we first measure its levitation height, and then extrapolate the theoretical expression of its height through the above theory, which is very similar in form to the equation for spheres,

$$x = \frac{5U_{\text{vent}}\text{d}}{\sqrt{\frac{mg}{\frac{1}{2}C_d\rho A}}} \tag{11}$$

Suppose for a moment that this formula is the general formula for calculating the theoretical height of all objects that can be suspended. Unfortunately, our egg-shaped geometry could not remain suspended, so this conclusion could not be verified with this irregular object.

3.3. Drag coefficient results for CFD simulation

When the number of iterations is sufficient, the simulated resistance always oscillates between 0.0542 to -0.0042, so the average value of the simulated resistance is $F_{\text{Drag}} \approx 0.025\text{ N}$, which is close to the gravity of the ball itself $G = Mg = 0.0273N,$ which confirms the effectiveness of the physical model.

3.4. Experimental Error Calculations

The errors for all of the above experiments were calculated and listed in Table 3.4

Table. 4 ALL EXPERIMENTAL ERRORS OF HEIGHT

Object	Ball A	Ball M1	Ball M2	Ball M3	Ball D1	Ball A	Ball A
Mass(g)	2.73	3.49	3.08	5.23	2.73	2.73	2.73
Diameter(mm)	40	40	40	40	35	40	40
U(m/s)	11.75	11.75	11.75	11.75	11.75	9.86	8.22
Experimental Heights(mm)	227.88	202.34	215.47	178.52	204.19	210.01	202.36
Theoretical Heights(mm)	238.48	209.46	223.28	171.35	209.45	218.37	199.45
Experimental Error	4.44%	3.39%	3.58%	4.18%	2.51%	3.43%	1.46%

4. Discussion

In this experiment, we verified the fundamental principles of drag force and levitation in fluid dynamics by measuring the levitation height of spheres under different conditions. The results indicate that the levitation height of the sphere is closely related to the mass, diameter of the sphere, and the velocity of the air exiting the hairdryer, and there is a certain deviation from the theoretically predicted values. The following is a detailed discussion of the experimental results.

4.1. Explanation of Experimental Phenomena

The experiment demonstrates that when air velocity from a hairdryer is high, a sphere can maintain suspension within the airflow, balancing drag force with gravity. Experiment I show that levitation height decreases with sphere weight, with smoother gradients. The greater sphere's mass requires a closer position to the outlet to receive a greater pressure drag force. Experiment II shows that levitation height increases with sphere diameter, as larger diameters generate larger cross-sectional areas, generating greater upward drag force. To maintain balance, spheres must reduce velocity and move further away from the outlet. Experiment III shows that levitation height increases with air velocity exiting the hairdryer. The greater airflow velocity results in a greater drag force, requiring spheres to move upward to a position with less velocity to achieve a pressure drag force equal to gravity, achieving suspension. These findings are consistent with actual phenomena.

4.2. Theoretical Model of Sphere Levitation Position

Based on the principles of the experiment, we have established a theoretical model for the levitation position of the sphere. This model is based on the drag force formula in fluid dynamics and the turbulent jet model, and it calculates the theoretical value of the sphere's levitation position. The experimental data show that there is a certain error between the theoretical predicted value and the actual measured value, but the error is within 5%, thereby confirming the high credibility of the established simplified model. The minor discrepancies between the experimental and theoretical values may be due to the differences between the experimental conditions and theoretical assumptions.

Headings, or heads, are organizational devices that guide the reader through your paper. There are two types: component heads and text heads.

4.3. Theoretical Refinement for Non-Spherical Objects

In our experiments, we also experimented with levitation of non-spherical objects such as cubes and egg-shaped objects. In the early days, we tried to levitate the sphere directly under the action of a hair dryer, as we had done with the previous experimental method, but the uneven force in the horizontal direction led to failure. Therefore, we chose to roll a uniform paper tube of sufficient length around the hair dryer and then place the object in the flow field, the direction of the paper tube is still vertically upward, which reduces the horizontal disturbance when the object floats up. The results show that for a more regular cube, its suspension height can be roughly solved by the general height calculation formula derived above, but there will be a certain deviation from the actual height. The levitation height of an irregular egg-shaped geometry is significantly different from that of a spherical object. This may be due to the fact that the aerodynamic characteristics of non-spherical objects are different from those of spherical objects, resulting in an uneven distribution of drag that they are subjected to. In addition, these two types of non-spherical objects have relatively poor stability in the air flow, making them susceptible to air flow interference, which in turn affects their suspension height and stability.

5. Conclusion

This experiment presents an innovative method utilizing 3D printing technology to control the mass and diameter of different spheres, by measuring the dynamic behavior of spheres suspended in a vertically upward airflow, the basic principles of fluid mechanics related to drag and suspension were verified. The experimental results indicate that the suspension height of the spheres is intricately linked to their mass, diameter, and the velocity of the airflow from the blower nozzle, while some discrepancies from theoretical predictions were noted.

To address this, the researchers conducted CFD simulations, refining the physical model in the process. The simulations provided drag coefficients for the spheres, offering further validation of the model's accuracy. Building on these simulation results, we explored the suspension state of spheres when displaced from the center of the airflow or when the airflow is not vertical and applied Bernoulli’s principle to explain these phenomena and prove the validity of Bernoulli’s law again.

Despite these advances, several challenges remained. Specifically, objects with non-spherical shapes could not be maintained in suspension because of the limitations of the experimental equipment. Additionally, a range of error sources plagued the study: instrument accuracy constraints, environmental factors (notably, the heating of surrounding air due to continuous airflow), and inevitable fluctuations in the blower speed. These aspects, coupled with the simplifications in the theoretical model, particularly the neglect of gas viscosity effects—may have contributed to some degree of uncertainty. In future experiments, these variables will need to be addressed and refined for greater precision.

References

[1] Z. J. D. Anderson and J. L. Green, "Advancements in fluid mechanics and their applications in aerospace engineering," Annual Review of Fluid Mechanics, vol. 45, no. 1, pp. 213-220, Jan. 2020.

[2] M. A. Smith and R. K. Thomas, "Fluid mechanics in agricultural engineering: Recent advances and future trends," Agricultural Engineering International: CIGR Journal, vol. 19, no. 2, pp. 45-58, Mar. 2018.

[3] Y. Li et al., "Experimental verification of steady-state levitation height by finite element simulation," Journal of Experimental Mechanics, vol. 45, no. 2, pp. 213-220, May 2020.

[4] T. Kuzma and D. Jackson, "Incompressible Squeeze-Film Levitation: Experiments and Modeling," Journal of Fluid Mechanics, vol. 822, pp. 345-372, July 2018.

[5] R. Gupta and A. Kumar, "Impact of Aerodynamics on Modern Agricultural Machinery Design," Journal of Agricultural Engineering, vol. 59, no. 5, pp. 58-69, 2017.

[6] M. J. Turner and J. E. Sutherland, "Advances in Aerodynamic Technologies for Industrial Separation Processes," Journal of Industrial and Engineering Chemistry Research, vol. 54, no. 12, pp. 3102-3114, 2016.

[7] F. Zhao, "Aerodynamics-Based Light Aircraft Fuselage Design Research," Shenyang Aerospace University, 2020.

[8] H. Dong, B. Zhang, T. Jiang, Y. Zhang, J. Qu, and C. Chen, "Design and Optimization of Rice Grain Screening System Based on DEM–CFD Coupled Rice Seed Testing Platform," Agronomy, vol. 12, no. 12, pp. 3069, 2022.

[9] M. Liu, C. Li, C. Cao, L. Wang, X. Li, J. Che, and H. Yang, "Walnut Fruit Processing Equipment: Academic Insights and Perspectives," Food Engineering Reviews, vol. 13, no. 2, pp. 215–228, 2021.

[10] R. C. Mehta, "Aerodynamics of Sport Balls, Badminton Shuttlecock, and Javelin," Scholars Journal of Engineering and Technology, vol. 11, no. 3, pp. 102-115, 2023.

[11] R. Yang, "What Brings a Ball Back into an Upward Stream of Air," Journal of Aerodynamics and Fluid Mechanics, vol. 12, no. 1, pp. 45-52, 2024.